Visual Inspection of Transparent Objects
Physical Basics, Existing Methods and Novel Ideas

Johannes Meyer

Vision and Fusion Laboratory
Institute for Anthropomatics
Karlsruhe Institute of Technology (KIT), Germany
johannes.meyer@kit.edu

Technical Report IES-2014-04

Abstract: Various industries, e. g., manufacturers of optical components or medical equipment, use components made out of transparent materials to craft devices for high-precision applications. As this involves the need for fulfilling high quality assurances, any kind of defect like enclosed air bubbles, contaminants or cracks, has to be reliably detected. Much effort has been spent and is currently spent into developing methods suitable for visually inspecting transparent objects. In contrast to opaque objects, transparent materials pose various challenging problems, as any light ray involved in the inspection process can be reflected and refracted by the investigated sample, complicating the design of the setup and of the method used for the inspection. On the one hand, this report gives an introduction to the specific physical properties of interest of transparent objects. On the other hand, it provides an overview over existing methods used for capturing these properties and describes sketches of some novel inspection approaches.

1 Introduction

The inspection of transparent objects is very important for various industries. For example, windshields and headlight glasses of automobiles have to be checked for cracks or impurities which might impair the sight of the driver or cause instabilities. In food industry, glass bottles or other food containers have to be checked for being impermeable and free from contaminants. Besides, plastic lenses used for laser-supported eye surgery have to be inspected to ensure certain quality requirements. Furthermore, optical elements themselves, as they are used in optical instruments, have to be inspected, in order to check whether they meet their specifications.

In contrast to transparent objects, there exist various methods suitable for inspecting opaque or specular objects. This report introduces the characteristic optical properties of transparent objects, discusses possible defects related to these properties and covers the corresponding challenges of inspection. Besides, rough sketches of some novel inspection approaches are presented.

2 Properties of Transparent Objects

As for any object, the properties of transparent objects can be divided into the two groups of optical properties and 3D geometry, which are presented in the following two sections.

2.1 3D Geometry

The 3D geometry of a transparent object refers to its outer shape. Depending on the object on hand and on the visual inspection task, the complete reconstruction of the object is required or differences between the test object and a reference object, e. g., defects, have to detected. For example, glass or plastic lenses used for optical imaging only produce the desired images if their 3D geometry exactly matches the specifications, which is why a complete reconstruction of their outer shape would be necessary for their inspection.

Common methods used for visually obtaining the geometry of opaque objects are based on triangulation, optical path lengths or intensity measurements. However, most of these methods cannot be directly applied to transparent objects, as most of the incident light is transmitted and nearly no light is reflected.

Triangulation approaches usually rely on the calculation of a missing side of the triangle consisting of a (laser) light source, the illuminated spot on the test object and the sensor observing the test object [Nol07]. The missing side is mostly the distance of the sensor and the current measurement spot on the test object. As the surface of a transparent object shows barely no reflections and transmits most of the incident light, there is no clearly visible illuminated spot that can be seen by the sensor. As this is also the case for any pattern projection or Moire method, triangulation is not suitable for obtaining the 3D geometry of transparent objects.

Methods based on measuring the length of the optical path of light (LIDAR [Cam02], interferometry [Har92], shearography [SY03], holography [Kre05]), which is sent to the object and which is observed after being reflected, also require the test object to reflect a certain amount of the incident light, which is why they are not suitable for transparent objects either.

In contrast, methods based on capturing the intensity of light transmitted by transparent objects might be suitable for obtaining the object's 3D geometry. One of these methods – the shape from silhouette approach – is described in section 3.1. However, it has yet not been used to acquire the 3D shape of transparent objects. Therefore, a simple but novel approach using shape from silhouette is presented in 4.1.

2.2 Optical Properties

Furthermore, also optical properties might be of interest. These include the refraction index and the color of the test object. Depending on the requirements of the actual application, the color of the transparent object, i. e., light of which wavelengths is absorbed or transmitted by the object can be determined by observing the light transmitted by the test object with a color camera or with a spectrally resolving sensor [Cha03]. As the visual appearance and the optical effects of transparent objects are mainly caused by light being deflected during transmission, the spatial distribution of the refraction index is of special importance.

Refraction occurs if light passes the boundary between two adjacent media with different refraction indices n_1 and n_2. If the angle of incidence of the incident light ray in medium 1 is denoted by θ_1 with respect to the normal of the boundary layer and if θ_2 is the corresponding angle of the emitted light ray in medium 2, Snell's law of refraction holds:

$$n_1 \sin\theta_1 = n_2 \sin\theta_2 \,.$$

The effect of refraction is illustrated in Fig. 2.1. If it is $\theta_1 = 0°$, it holds $\theta_2 = 0°$. For exact calculations, the refraction index has to be considered as a function of the light's wavelength λ:

$$n = n(\lambda) \,.$$

This dependency is called dispersion. If the material of the transparent object is inhomogeneous, the refraction index might even be a function of the position $\mathbf{x} \in \mathbb{R}^3$:

$$n = n(\lambda, \mathbf{x}) \,.$$

The refraction index can be measured, e. g., by means of the Schlieren imaging method described in Sect. 3.2.

Material defects affecting the refraction index can result in serious consequences: for example, small enclosed air bubbles or contaminants inside a transparent plastic lens used for a laser-supported eye surgery might cause the laser to be directed into the wrong direction and therefore to harm the patient. Such defects can be

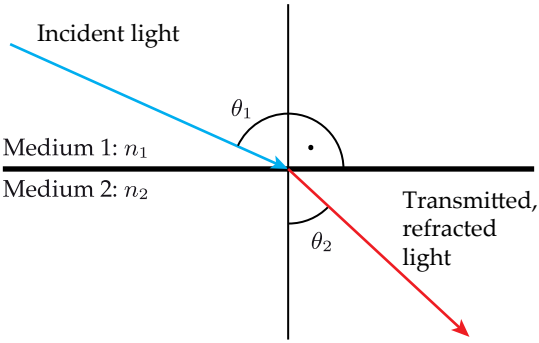

Figure 2.1: Snell's law of refraction.

detected as local inhomogeneities of the refraction index or as sources of scattered light if illuminated in dark field.

3 Existing Methods

In this section, two existing methods for inspecting transparent objects are presented. Besides their basic principle, also the drawbacks of the methods will be mentioned.

3.1 Shape from Silhouette

Shape from silhouette is a method which is able to approximate the 3D shape of opaque objects by combining views of its silhouette captured out of different projection directions [TCM+02]. To simplify matters, only two dimensions will be considered for explaining the approach. Figure 3.1 illustrates the setup for capturing an object's silhouette out of a single projection direction. As the light source is placed in the focal point of the lens L_1, the object is illuminated with parallel light, so that the object's silhouette is visible on the sensor. The setup is now rotated around the object in order to capture silhouettes out of multiple perspectives. As the rotation angles are known and the illumination is calibrated with respect to the sensor, the path of the two rays which are just 'touching' the borders of the object can be reconstructed and the rectangular area between these two rays can be intersected with the other rectangles corresponding to the different projection directions. By this means, a step-wise approximation of the outer shape of the

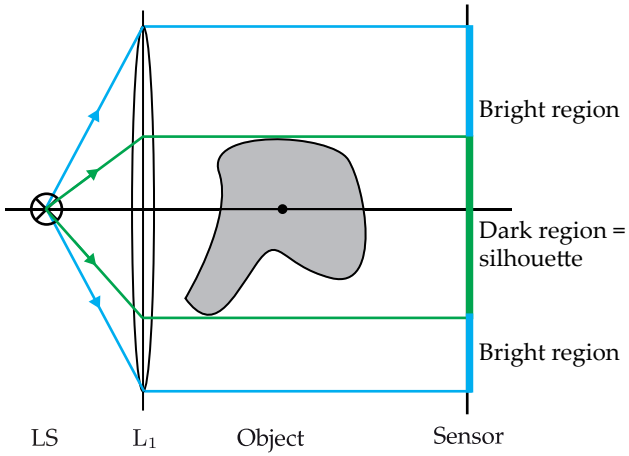

Figure 3.1: Visualization of the optical setup used for shape from silhouette. A light source LS is placed in the focal point of the lens L_1, so that only parallel light reaches the investigated object. As the object is opaque, its silhouette corresponding to the current projection direction is imaged to the sensor and appears as a dark region.

investigated object can be obtained (see Figure 3.2). The more projections directions are used the more exact the resulting approximation will be. As rectangles are convex geometric objects, an intersection of two rectangles will always result in another convex object [Cop98]. This is why – theoretically – shape from silhouette can only achieve a perfect reconstruction of convex objects and any concave structures on the surface of the investigated objects will never be contained in the reconstruction (see Figure 3.2).

In the three-dimensional case, the single two-dimensional projections are polygons, which do not necessarily have to be convex. The results of the corresponding intersections can be arbitrary polyhedra that do not have any inner structures like cavities. Unfortunately, the intersection of three-dimensional polyhedra is very complex and computationally expensive. Besides, as it is presented here, shape from silhouette gives much better results for opaque objects than for transparent objects, as only the contours of transparent objects would be visible as slightly darker structures on the sensor. In Sect. 4.1, an approach is proposed which possibly resolves this drawback.

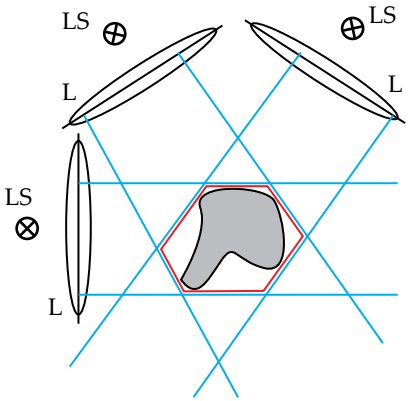

Figure 3.2: The setup shown in Fig. 3.1 is used for multiple projection directions. For every configuration, the two rays touching the object are colored blue. The red polygon, which is the intersection of the rectangular areas between the pairs of rays, presents a convex approximation of the shape of the investigated object.

3.2 Schlieren Imaging

As mentioned above, light rays do not follow a straight line when passing a transparent object with varying refraction index. As this effect can be measured, information about the refraction index can be gained [Sch95]. In order to obtain an intensity image representing the deflection of the rays, a so-called schlieren stop can be used, which is placed asymmetrically into the optical path. By this means, the deflection of the light rays results in a varying intensity on the image sensor. Figure 3.3 shows the principal setup used for schlieren imaging. The setup is sensitive for changes of the refraction index perpendicular to the edge of the schlieren stop. In order to obtain information about different directions of the gradient of the refraction index, images with different configurations of the schlieren stop have to be captured or a color wheel can be placed in the focal point of L_2, which allows a color encoding of the deflection direction.

Another variant of schlieren imaging uses a certain '4D' background illumination, which utilizes micro lenses in order to achieve a color encoding of the spatial position of each illuminating element and of the outgoing direction. By this means, the test object can be placed just in front of this background and common consumer cameras can be used to obtain a qualitative schlieren image [WRH11].

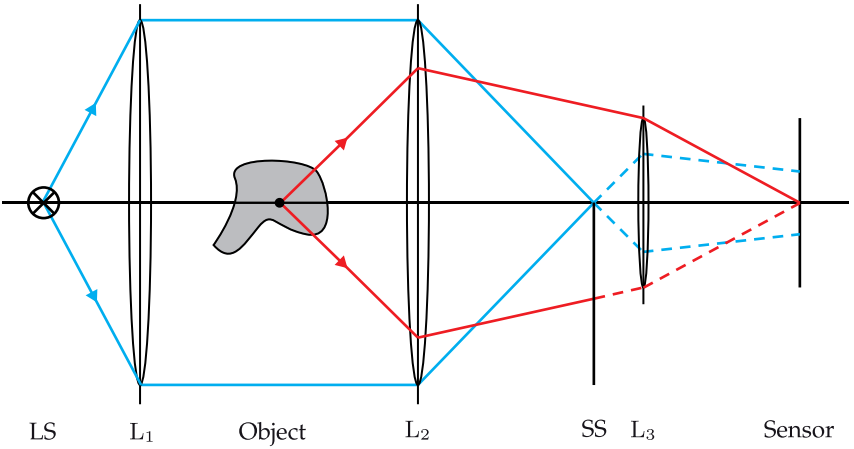

Figure 3.3: Principle of schlieren imaging. The light of the light source LS is collimated by L_1 and illuminates the investigated transparent object. The collimated light is focused by the lens L_2. A schlieren stop SS is located in the focal point of L_2, ideally halving the luminance if no test object is present. Light rays deflected upwards (downwards) by the test object are able to pass the schlieren stop (are blocked) and result in high (low) values output by the sensor. The resulting intensity images are called 'schlieren'. By means of the lenses L_2 and L_3, a focused imaging of the object onto the sensor is realized.

As already mentioned, a single configuration of the original schlieren setup only allows to obtain information about the components of the refraction index distribution, which are perpendicular to the edge of the schlieren stop. Section 4.2 outlines a novel approach which could possibly resolve this drawback.

4 Novel Approaches

In this section, two novel ideas are presented, which extend the methods shape from silhouette and schlieren imaging to better suit transparent objects.

4.1 Shape from Silhouette for Transparent Objects

As discussed in Sect. 3.1, the shape from silhouette method is not directly suitable for obtaining the outer shape of transparent objects. The problem is, that the

inspected object should be opaque, so that its silhouette is represented by a thorough, dark region on the image sensor. The contrast with which the contour of a transparent object would be visible, might be low, resulting in inaccurate silhouette measurements.

Figure 4.1 shows the sketch of a setup which could possibly be used to capture the single silhouette projections of transparent objects. The original setup from Fig. 3.1 is extended by another lens and a telecentric stop which is placed in this lens' focal point. By this means, only rays running parallel to the optical axis between the two lenses are able to pass the telecentric stop and to reach the image sensor. Any ray running through the transparent object will be refracted when entering or leaving the object or when traversing inner structures of the object, so that it will not be parallel to optical axis anymore and will be blocked by the telecentric stop. The image formed on the sensor should show the silhouette of the object corresponding to the configured projection direction. By utilizing this setup, the shape from silhouette method (Sect. 3.1) should be applicable to transparent objects as well as to opaque objects. However, there still are some transparent objects which could be problematic for this method, e. g., a transparent cuboid which is arranged so that its sides are exactly parallel or perpendicular to the optical axis resulting in no refraction of some of the rays and therefore in an unusable sensor image. But as this case is very unlikely and as objects are rotated during the inspection, the approach could still be successful for such object classes.

4.2 Variable Stop Schlieren Imaging

As mentioned in Sect. 3.2, the schlieren method can be used to visualize the refraction index of transparent objects as intensity images. However, the method is only sensitive for refraction index gradients perpendicular to the edge of the schlieren stop as it is aligned in the current setup.

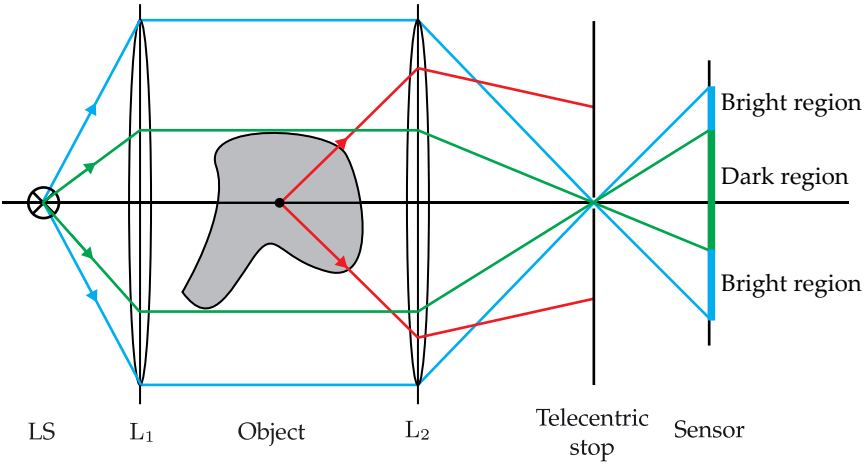

Figure 4.1: A setup allowing to apply shape from silhouette to transparent objects. The setup from Fig. 3.1 is extended by an additional lens L_2 and a telecentric stop which is placed in the focal point of L_2. By this means, only rays parallel to the optical axis are able to reach the sensor and any ray coming in contact with the transparent object and getting refracted will be blocked by the telecentric stop.

By using a highly variable and controllable schlieren stop and by acquiring an image series whose images correspond to the configurations of the schlieren stop, the refraction index field could possibly be sampled. Figure 4.2 illustrates a possible setup. Here, a so-called digital micromirror device (DMD) is used to realize the variable schlieren stop. A DMD is a rectangular array of for example $2 \cdot 10^6$ mirrors having a size of about $10\mu\text{m} \cdot 10\mu\text{m}$ [Ins15]. Every single mirror can be electrically tilted by several discrete angles with a frequency of 400 MHz. By this means, the single elements can be turned 'on' or 'off', i. e., they can be set to direct the light in the correct direction towards L_3 or out of the optical system. Thus, the DMD can be used to realize various stop configurations and a series of images containing information about the refraction index gradients in the corresponding direction can be acquired.

5 Conclusion

This report introduced the physical basics regarding the visual inspection of transparent objects and the associated challenges. The suitability of existing visual inspection methods for the inspection of transparent objects has been discussed and

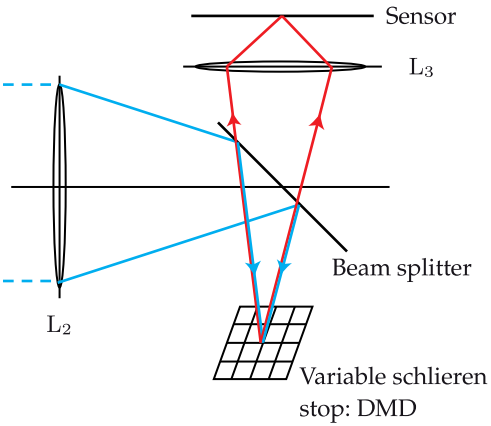

Figure 4.2: Principle of schlieren imaging realizing a variable schlieren stop. The figure has to be considered as an extension of the part right from the lens L_2 in Figure 3.3. To simplify matters, the deflected rays are neglected. Here, a beam splitter is placed in the optical path beyond the lens L_2. After being reflected by the beam splitter, the light reaches a digital micromirror device (DMD), which replaces the schlieren stop of the original setup. This DMD is controlled by a computer to realize different schlieren stop configurations $S_1, S_2, \ldots, S_N$ at different points of time $t_1, t_2, \ldots, t_N$. The sensor is triggered to acquire images $I_1, I_2, \ldots, I_N$ at the respective points of time t_i.

two novel ideas have been presented: on the one hand, an image acquisition setup has been proposed, which possibly allows the application of shape from silhouette to transparent objects and on the other hand, an expansion of the schlieren method has been presented, which utilizes a variable schlieren stop in order to gain more information about the investigated object.

Now, these approaches need to be physically realized and evaluated by means of theoretically well-grounded experiments.

Bibliography

[Cam02] James B. Campbell. *Introduction to remote sensing*. Guilford Press New York, 3rd edition, 2002.

[Cha03] Chein-I Chang. *Hyperspectral imaging : techniques for spectral detection and classification*. Kluwer Academic, 2003.

[Cop98] William A. Coppel. *Foundations of convex geometry*. Australian Mathematical Society lecture series ; 12. Cambridge University Press, 1st edition, 1998.

[Har92] Parameswaran Hariharan. *Basics of interferometry*. Academic Press, 1992.

[Ins15] Texas Instruments. *DLPS025B, http://www.ti.com/lit/ds/symlink/dlp9500.pdf*, 2012 (accessed January 7, 2015).

[Kre05] Thomas Kreis. *Handbook of holographic interferometry : optical and digital methods*. WILEY-VCH, 2005.

[Nol07] Reinhard Noll. Lasertriangulation. In Norbert Bauer, editor, *Handbuch zur Industriellen Bildverarbeitung*, pages 56–60. Fraunhofer IRB Verlag, Stuttgart, 1st edition, 2007.

[Sch95] Alexander Schwarz. *Multitomographische Temperaturmessung in Flammen mit einem Schlierenmeßaufbau*. PhD thesis, Universität Karlsruhe (TH), 1995.

[SY03] Wolfgang Steinchen and Lianxiang Yang. *Digital shearography : theory and application of digital Speckle pattern shearing interferometry*. SPIE Optical Engineering Press, 2003.

[TCM+02] Marco Tarini, Marco Callieri, Claudio Montani, Claudio Rocchini, Karin Olsson, and Therese Persson. Marching intersections: An efficient approach to shape-from-silhouette. In *VMV*, pages 283–290, 2002.

[WRH11] Gordon Wetzstein, Ramesh Raskar, and Wolfgang Heidrich. Hand-held schlieren photography with light field probes. In *Computational Photography (ICCP), 2011 IEEE International Conference on*, pages 1–8. IEEE, 2011.